Convertible and conformationally constrained nucleic acids (C 2 NAs)

Jean-Marc Escudier, Corinne Payrastre, Béatrice Gerland, Nathalie Tarrat

Convertible and Conformationally Constrained Nucleic Acids (C_2NAs)

Escudier Jean-Marc,*[a] Payrastre Corinne,[a] Gerland Béatrice [a] and Tarrat Nathalie [b]

We introduce the concept of Convertible and Constrained Nucleic Acid (C_2NA). By means of the synthesis of a stereocontrolled *N*-propargyl dioxo-1,3,2-oxaza-phosphorinane as internucleotidic linkage, the torsional angles α and β can adopt either the canonical (g^-, t) set of values able to increase DNA duplex stability or the non-canonical (g^+, t) set that stabilized hairpin structure when installed within the loop moiety. With an appended propargyl function on the nitrogen atom of the six-membered ring, the copper catalysed Huisgen's cycloaddition (CuAAC click chemistry) allows for the introduction of new functionalities at any location on the nucleic acid chain while maintaining the properties brought by the geometrical constrain and the neutral internucleotidic linkage.

Introduction

Nucleic acid molecules exhibit an increasing importance in the context of therapeutics, molecular diagnostics and nanotechnologies.[1] For these purposes, chemists have developed modifications of their inner nucleotide components in order to improve their bio-stability, their target affinity or their ability to be decorated by new functionalities such as fluorescent labels or any other molecules able to explore new applications.[2] In that context, the most efficient modification was the restriction of the conformational space of the sugar moiety in its C3'-*endo* conformation in order to mimic the geometry adopted in RNA duplex.[3] Locked Nucleic Acid (LNA) in which the δ torsional angle (Figure 1) is completely frozen, is to date the best element of this class of conformationally constrained nucleotides.[4] Concerning the decoration of oligonucleotides (ODNs) by extra functionalities, the copper catalysed azide-alkyne cycloaddition (CuAAC) appeared to be a very powerful approach.[5] These considerations taken together, the Wengel's group proposed an amino-LNA with an appended alkyne function. This RNA nucleotide mimic could be denoted as a convertible and locked nucleotide that exhibited extensive properties and applications.[6]

Based on the concepts of preorganization[7] and of convertible approach,[8] we engaged in two parallel programs. The first was directed towards the development of nucleotides in which the sugar/phosphate backbone geometry was constrained (Constrained Nucleic Acids: CNAs) in order to propose nucleotides analogues able to fit either with the B-DNA canonical structure or others non-helical relevant disparate secondary structures.[9] The second research axis was oriented towards the design of convertible nucleotides where an appended arm at the C5' position was bearing an orthogonally reactive function such as an alkyl halide or alkyne.[10] Here we present our effort to merge these two approaches in the development of a combination of the two properties into one family of dinucleotides: the Constrained and Convertible Nucleic Acid (C_2NA).

The most prominent members of the CNA family are the α,β-D-CNA in which the conformational control of the torsional angle α and β of the nucleic acid sugar/phosphate backbone was achieved by introduction of a 1,3,2-dioxa-phosphorinane ring connecting one oxygen atom of the phosphate moiety to the 5'-carbon of the deoxyribose.[11] When featuring the canonical set of values *gauche(-)/trans*, α,β-D-CNA are perfect B-DNA nucleotide mimics and induce a strong stabilization of duplex structure[12] whereas stability of hairpin or bulge structures can be modulated by using α,β-D-CNA featuring a *gauche(+)* conformation of the α angle, located in the unpaired moiety of the secondary nucleic acid structure.[13]

Since we wanted to keep the D-CNA's general scaffold for their interesting stabilization effects for the newly designed C_2NA and because the C5'-carbon was no longer available for further functionalization, we chose to investigate the replacement of one oxygen atom within the dioxa-phosphorinane ring by a nitrogen atom properly alkylated by a propargyl function in order to bring the convertible ability. It was also of importance to keep the natural C5'-O5'-P-O3' bonds unchanged to prevent any change into the internucleotidic length and local geometry. Therefore, it turned out that one of the non-bridging oxygen of the phosphate was formally suitable to be replaced by the propargyl amino group to design dioxo-1,3,2-oxaza-phosphorinane as scaffold for the development of C_2NA (Figure 1).

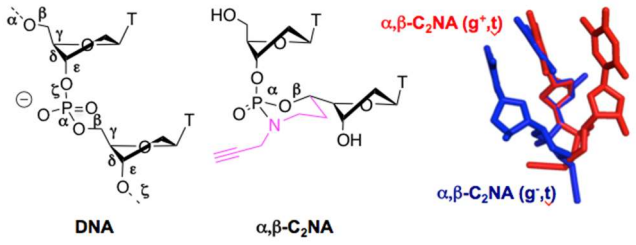

Fig. 1. Left: the six backbone torsion angles (labelled α to ζ) of nucleic acids. Middle: the constrained and convertible dinucleotide in which α and β are stereocontrolled by a dioxo-1,3,2-oxaza-phosphorinane ring structure bearing a clickable propargyl function (α,β-C_2NA). Right: superimposition of minimized structures of ($S_{C5'}$, S_P) α,β-C_2NA TT (red)

[a] *Laboratoire de Synthèse et Physico-Chimie de Molécules d'Intérêt Biologique, UMR CNRS 5068, Université Paul Sabatier, 118 route de Narbonne, 31062 Toulouse, France.*
E-mail: escudier@chimie.ups-tlse.fr.
[b] *CEMES, Université de Toulouse, CNRS, 29 rue Jeanne Marvig, Toulouse 31055, France.*

Electronic Supplementary Information (ESI) available: NMR spectra of described compounds, mass spectrometry data of ODNs, thermal denaturation curves, typical HPLC profile for CuAAC conjugation. See DOI: 10.1039/x0xx00000x

and ($R_{C5'}$, R_P) α,β-C_2NA TT (blue) with featuring a non-canonical *gauche(+)* and canonical *gauche(-)* configuration, respectively.

In this paper, we present the *in silico* calculations that ascertain the synthesis of the appropriate regio-isomer of the oxaza-phosphorinane towards the best α,β-C_2NA design. The rapid synthesis of both diastereoisomers of α,β-C_2NA phosphoramidites by *H*-phosphonate chemistry and their structural determination by means of NMR spectroscopy are described. Next, we show that α,β-C_2NAs can be efficiently incorporated within oligonucleotides and exhibit stabilizing properties of nucleic acid secondary structures (duplex, hairpin and bulges). Eventually, as a proof of concept, we report the conjugation of oligonucleotides including α,β-C_2NAs with fluorescein through copper catalysed Huisgen's cycloaddition.

Results and discussion

In silico α,β-C_2NA structure conformational study

As previously observed with α,β-CNAs,[9, 12, 14] among the four possible α,β-C_2NAs isomers, only two of them can have all the substituents of the phosphorinane ring in the orientation that favours their formation, stability and conformational interest: the upper nucleoside in the apical position, the exocyclic oxygen and the lower nucleoside in equatorial position. Moreover in line with the results obtained with their α,β-CNA analogues, a simple molecular model examination indicated that this couple should mainly differ on the α torsional angle conformation.[11] Therefore we focused the *in silico* conformational investigation on these two potentially major diastereoisomers of α,β-C_2NAs, *i.e.* the ($S_{C5'}$, S_P) α,β-C_2NA (**3** in its 5'-O and 3'-O unprotected form, Scheme 1) and ($R_{C5'}$, R_P) α,β-C_2NA (**11** in its 5'-O and 3'-O unprotected form, Scheme 2). The accessible conformation space of the two compounds was explored through *ab initio* molecular dynamics simulations (AIMD) followed by quenches. AIMD were done starting from different initial conformations. The total AIMD trajectory length was 18 ps for ($S_{C5'}$, S_P) α,β-C_2NA and 12 ps for ($R_{C5'}$, R_P) α,β-C_2NA (with a time step of 1.5 fs), the associated average temperatures of the trajectories being respectively 543K and 545K. Thirty five structures were extracted by dividing the trajectories into equal intervals.

After their geometry optimizations, the energy of the structures was located within a range of 11.0 kcal.mol-1 and 9.6 kcal.mol-1 for ($S_{C5'}$, S_P) α,β-C_2NA and ($R_{C5'}$, R_P) α,β-C_2NA, respectively. The most stable conformation of the ($R_{C5'}$, R_P) isomer was found to be 1.4 kcal.mol-1 below the one of the ($S_{C5'}$, S_P) isomer (Figure 2).

In both optimized dinucleotides, the puckering of the upper sugar unit is C2'-endo and the oxaza-phosphorinane ring exhibits a chair conformation. However, the two structures differ in the conformation of the lower sugar unit: C2'-endo for ($R_{C5'}$, R_P) α,β-C_2NA and C3'-endo for ($S_{C5'}$, S_P) α,β-C_2NA. A W-shaped P-O5'-C5'-C4'-H4' structure is observed for the two compounds, a geometrical feature that will be confirmed by the NMR study (in agreement with the observed long range 4JH/P coupling constants). Interestingly, the distances between the branching points of the dinucleotide (5'-O of the upper nucleotide and 3'-O of the lower) differ by 2.1Å (8.5Å for ($S_{C5'}$, S_P) α,β-C_2NA and 10.6Å for ($R_{C5'}$, R_P) α,β-C_2NA), and those between the bases centres by 1.3Å (4.9Å and 3.6Å, respectively). The latter certainly explains in large part the energy difference between the two diastereoisomers by the loss of the stabilizing stacking interaction for ($S_{C5'}$, S_P) α,β-C_2NA whereas the conformation of ($R_{C5'}$, R_P) α,β-C_2NA is highly favourable. Another important structural point is that compound ($S_{C5'}$, S_P) α,β-C_2NA exhibits an orientation flip of its upper sugar ring, a phenomenon that appears in loop moiety of hairpin structure. All these features outlined by the simulation indicate that ($R_{C5'}$, R_P) α,β-C_2NA should be well adapted to fit with a duplex structure whereas ($S_{C5'}$, S_P) α,β-C_2NA should be better integrated within unpaired structure such as loop.

Concerning the clickable propargyl function, one can notice that it is easily accessible by an external molecule in both cases. The partial charges of the propargyl carbon atoms are similar in both isomers: -0.3 on the carbon bound to the nitrogen atom, 0.0 on the central carbon and -0.2 on the final one. It indicates that if a reactivity difference would be observed once introduced into extended oligonucleotides, it would belong to the accessibility and not to the charges of the function.

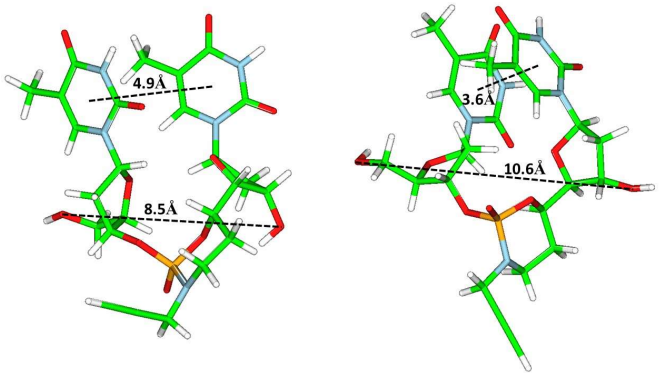

Fig. 2. Most stable conformations issued from the *in silico* protocol. Left: Dinucleotide ($S_{C5'}$, S_P) α,β-C_2NA (**3** in its unprotected form). Right: Dinucleotide ($R_{C5'}$, R_P) α,β-C_2NA (**11** in its unprotected form).

Synthesis of α,β-C_2NA

The key intermediates in the synthetic pathway of α,β-C_2NAs are the 5'-C-propargylaminoethyl thymidines **2** and **10** that are epimers at the 5'-carbon of the sugar moiety of the nucleoside (Scheme 1 and 2). They are both obtained in moderate to good yield by displacement by the propargylamine of a tosylate group of tosyloxyethyl thymidines **1** and **9**, respectively, both previously described in the preparation of α,β–D-CNAs.[14]

Thanks to the methodology elaborated by A. Kraszewski and collaborators in the early 90's, preactivation of the thymidine H-phosphonate monoester by pivaloyl chloride led to a dipivaloyl phosphite that can react with the amino alcohol derivative to form a cyclic phosphoramidite intermediate, further oxidized in situ by water after addition of iodine that provided the oxaza-

phosphorinane.[15] This procedure led in average yield of 80% from 5'-C(S)-propargylaminoethyl thymidine **2** to a 2:1 ratio of diastereoisomeric oxaza-phosphorinane dinucleotides α,β-C_2NAs **3** and **4**, determined by ^{31}P NMR (δ= 2.4 and 4.7 ppm for **3** and **4**, respectively, Scheme 1).

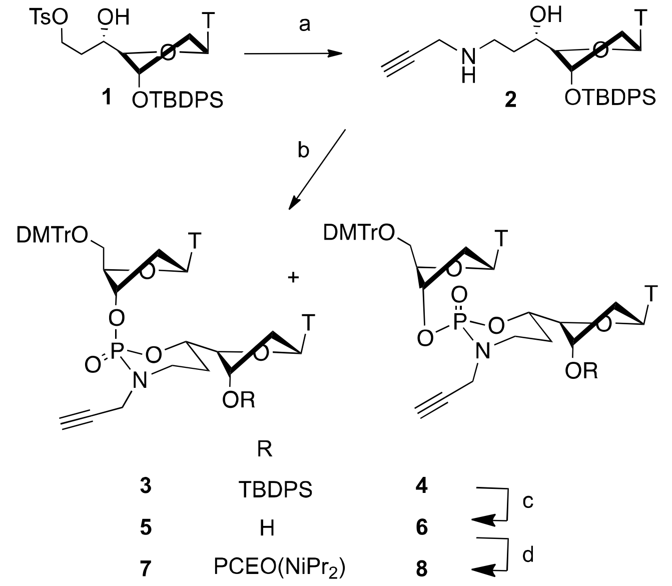

Scheme 1. Synthesis of ($S_{C5'}$, S_P) α,β-C_2NA and ($S_{C5'}$, R_P) α,β-C_2NA. a- Propargylamine, *i*Pr_2NEt, DMF, 65%. b- 5'-*O*-DMTr Thymidine *H*-phosphonate triethylammonium salt, PivCl, Pyr then I_2, 80%. c- TBAF, THF, 85-90%. d- 2-cyanoethoxydi*iso*propylamino chlorophosphine, *i*Pr_2NEt, THF, 87-95%.

A similar result was obtained from the epimeric propargylaminoethyl thymidine **10** with a slightly higher diastereoselectivity of 3:1 in favour of α,β-C_2NA **11** (^{31}P NMR δ = 2.7 ppm) over **12** (^{31}P NMR δ = 3.2 ppm) that appeared to be rather unstable under chromatographic conditions, explaining the modest overall yield of 60% (Scheme 2). In both cases, the major compounds formed were depicted at lower chemical shift in ^{31}P NMR with respect to their corresponding isomer (Δδ [illegible], which suggested the formation of the most stable chair conformation of the oxaza-phosphorinane as expected and previously observed during α,β-D-CNAs synthesis.[16]

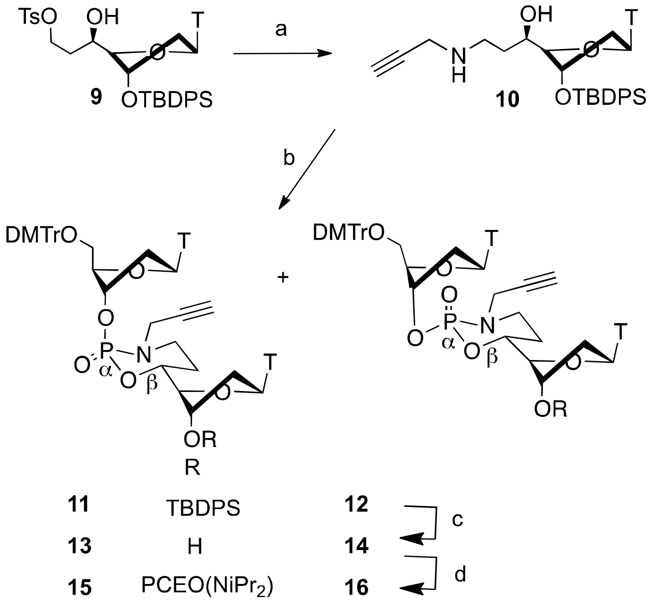

Scheme 2. Synthesis of ($R_{C5'}$, R_P) α,β-C_2NA and ($R_{C5'}$, S_P) α,β-C_2NA. a- Propargylamine, *i*Pr_2NEt, DMF, quant. b- 5'-*O*-DMTr Thymidine *H*-phosphonate triethylammonium salt, PivCl, Pyr then I_2, 60%. c- TBAF, THF, 85-87%. d- 2-cyanoethoxydi*iso*propylamino chlorophosphine, *i*Pr_2NEt, THF, 72-94%.

NMR structural study of C_2NA

When compared with their analogues α,β-D-CNAs, the α,β-C_2NAs differ by the replacement of an oxygen atom by a nitrogen within the phosphorinane ring and obviously, by the appended propargyl arm in between the two nucleosides. These differences could induce a dramatic change of conformational behaviour. Therefore, the analysis of the conformation of this new family of constrained nucleotides was carried out using ^{1}H, ^{13}C, ^{31}P and 2D NMR techniques, in order to determine the sugar puckering preference of each deoxyribose and the geometry of the oxaza-phosphorinane ring.

Sugar Puckering

By measuring the coupling constants exhibited by the protons of the 2'-deoxyribose moieties in ^{1}H NMR spectra of α,β-C_2NAs **3**, **4**, **11** and **12**, a rough evaluation of the sugar puckering can be estimated by the Altona and Sudaralingam's equation: %South = $[J_{H1',H2'}/(J_{H1',H2'} + J_{H3',H4'})] \times 100$,[17] with the results reported in Table 1.

All the 2'-deoxyribose moieties of α,β-C_2NAs exhibited the South conformation (C2'-*endo*) as expected for DNA constituents. However, it is noteworthy that the upper sugars of the major isomers **3** and **11** were pushed strongly towards the south conformation in comparison with the lowers units and with the standard puckering adopted within DNA. This favoured conformation can be associated with the neutral internucleotidic linkage featured by C_2NA that is known to enforce the C2'-*endo* puckering even in the case of ribose moieties.[18] Therefore, neither the oxaza-phosphorinane nor the

appended propargyl arm within α,β-C_2NAs have modified the sugar geometry with respect to their α,β-D-CNAs analogues.

Table 1. H/H coupling constants (Hz) of 2'-deoxyribose moieties in the ^{1}H NMR spectra (500 MHz) of α,β-C_2NA dinucleotides ($S_{C5'}$, S_P) **3**, ($S_{C5'}$, R_P) **4** and ($R_{C5'}$, R_P) **11**, ($R_{C5'}$, S_P) **12**.

α,β-C_2NA	sugar	Coupling constant *J* (Hz)					% South
		J(1',2')	*J*(1',2")	*J*(2',3')	*J*(2",3')	*J*(3',4')	
3	upper	5.5	10.0	0	5.0	<1	90
	lower	5.0	9.5	0	5.5	<1	85
4	upper	6.0	8.0	2.0	5.5	2.3	72
	lower	6.0	8.0	2.5	7.0	2.5	70
11	upper	5.4	8.7	2.0	4.8	<1	85
	lower	6.0	8.7	nd	5.4	1.8	77
12	upper	5.7	9.3	nd	5.1	<1	85
	lower	5.4	9.3	nd	5.1	2.7	66

Oxaza-phosphorinane ring conformation

The conformation of six membered ring including phosphorus and two oxygen or nitrogen (phosphorinane) can be determined by examining the $J_{H/P}$ coupling constants in ^{1}H NMR spectra of the proton within the cyclic structure. Gorenstein showed that when $^3J_{H/P}$ < 3 Hz, the considered proton can be assigned to be in an axial position and when $^3J_{H/P}$ > 20 Hz the proton adopts an equatorial position. This taken into consideration and together with the relative ^{31}P NMR chemical shift depicted for the phosphorus in each couple of diastereoisomers (the lower chemical shift belongs to a phosphorus with the oxygen in equatorial position on the phosphorinane ring), the absolute configuration of phosphorus can be assigned accordingly.[19]

On the other hand, Altona proposed that the torsional angle ε was correlated with $^3J_{H/P}$ of the 3'-proton according to the relation: ε = -θ -120°, where θ is obtained from $^3J_{3'\text{-}H/P}$ = 15.3 $\cos^2\theta$.[20]

Therefore, we collected and reported in Table 2 all the measurable $J_{H/P}$ coupling constant values in ^{1}H NMR spectra for α,β-C_2NAs **3**, **4**, **11** and **12**.

It is clear that the major isomers ($S_{C5'}$, S_P) α,β-C_2NA **3** and ($R_{C5'}$, R_P) α,β-C_2NA **11** present the oxaza-phosphorinane ring in a pure chair conformation with the 5'b- and 7'b-protons exhibiting constant values in agreement with axial positions whereas the 7''b-protons were depicted with large constants of 24 and 22 Hz, respectively, evidencing their equatorial positions. With average $^3J_{H/P}$ constant values, the minor isomers **4** and **12** appeared to fit with an oxaza-phosphorinane structure in slightly twisted chair conformation. This less stable conformation could explain the relative instability that became apparent upon standing for the minor isomer ($R_{C5'}$, S_P) α,β-C_2NAs **12**. Knowing the geometry adopted by the internucleotidic linkage gave an access to the torsional angle values of α and β (Table 3) by a simple molecular models examination. The ($S_{C5'}$, S_P) α,β-C_2NA **3** featured a non-canonical (*gauche(+), trans*) combination whereas ($R_{C5'}$, R_P) α,β-C_2NA **11** fitted with the conformation (*gauche(-), trans*) observed in B-DNA.

The observed $^3J_{H3'a/P}$ coupling constants were in the same range of value (7.5 ± 0.5 Hz, Table 3) and the calculated ε torsional angles were found to be in the *trans* conformation for all the α,β-C_2NAs isomers which was very similar to the one found in the corresponding α,β-D-CNAs.

Table 2. H/P coupling constants (Hz) in the 1H NMR spectra (500 MHz) of α,β-C_2NA dinucleotides **3**, **4** and **11**, **12**.

α,β-C_2NA	Coupling constant *J* (Hz)				
	J(5'b/P)	*J*(7'b/P)	*J*(7"b/P)	*J*(3'a/P)	*J*(4'b/P)[a]
3	<1	<1	24.0	8.0	5.5
4	2.0	8.5	12.0	7.2	4.0
11	<1	<1	22.0	6.9	3.6
12	2.1	nd	15.0	7.2	5.4

[a] Protons denoted as "a" belong to the upper nucleoside whereas those denoted as "b" belong to the lower nucleoside including the phosphorinane moiety.<w

Eventually, long range $^4J_{H/P}$ coupling constants were observed for all the α,β-C_2NAs isomers between the 4'-H of the downstream nucleoside and the phosphorus atom. A W-shaped P-O5'-C5'-C4'-H4' arrangement can explain these observations and provided an access to the value of the torsional angle γ, considering the sugar south conformation and each oxaza-phosphorinane chair or twist-chair geometry (Table 3). The main isomers **3** and **11** adopted a *gauche(+)* conformation for γ, when the minors were slightly distorted to the *cis(+)*. Therefore ($R_{C5'}$, R_P) α,β-C_2NA **11** appeared to be an interesting conformationally locked B-type analogue with four of its torsional angles in the same range than those observed for nucleotide involved in B-duplex.[21]

Table 3. Estimated α, β, γ ε torsional angle values of α,β-C_2NA dinucleotides **3**, **4** and **11**, **12**.

α,β-C_2NA	Torsional angle[a]			
	α	β	γ	ε[b]
3 ($S_{C5'}$, S_P)	g^+	t	g^+	t
4 ($S_{C5'}$, R_P)	t	t	c^+	t
11 ($R_{C5'}$, R_P)	g^-	t	g^+	t
12 ($R_{C5'}$, R_P)	t	t	c^+	t

[a] The following staggered pattern of the torsional angles is used: cis= 0 ±30° (c), gauche(+)= 60 ±30° (g^+), trans= 180±30° (t), gauche(-)= 300 ±30° (g^-). [b] angle α (C5'-O5'-P-O3'), angle β (C4'-C5'-O5'-P), and angle γ (C3'-C4'-C5'-O5') estimated from NMR data, angle ε (C4'-C3'-O3'-P) calculated from the Altona relation.

Oppositely, ($S_{C5'}$, S_P) α,β-C_2NA **3** differed from the canonical set of torsional angle value with α that was pushed by 120° from *gauche(-)* to *gauche(+)* conformation, this distortion was outlined at the turning phosphate position within loop moiety of hairpin structure and also appeared within bended DNA involved in protein/DNA complexes.[22]

Thermostabilty of α,β-C_2NA within duplex, hairpin and bulge structures

In order to evaluate the impact on DNA secondary structures formation ability of the newly synthesized convertible and constrained dinucleotide units α,β-C_2NAs featuring either the non-canonical or the canonical set of torsional angle conformation, the corresponding phosphoramidites derivatives **7** and **15** (Schemes 1 and 2) were used during automated synthesis of oligonucleotide according to the phosphoramidite technology.[23]

The following oligonucleotide sequences have been chosen to have a direct comparison of the melting temperature with those previously measured with the same constraint brought by the α,β-□□CNA analogues in order to have an insight of the influence of the appended propargyl function. Duplex 5'-GCGCTTGCCG/3'-CGCGAACGGC (**ODN 1**) has been modified on the TT step with the application of the *gauche(-)* or the *gauche(+)* constraint to the alpha torsional angle (Table 4, **ODN 2** and **7**).[24] Duplexes 5'-CGTTTTTTGCT/3'-GCAAAAAACGA (**ODN 3**) have been designed to study the influence of the *gauche(-)* constraint location by moving the modified α,β-C_2NA TT along the chain (Table 4, **ODN 4**, **5** and **6**).[25] A four thymidine-looped hairpin (**ODN 8**) has been modified with α,β-C_2NA TT featuring the *gauche(+)* constraint embedded at all the possible positions within the unpaired loop moiety (Table 4, **ODN 9**, **10**, **11** and **12**).[26]

Eventually, bulges have been constructed with the *gauche(+)* constraint within the loop or opposite to the loop using the α,β-C_2NA TT modified sequence **ODN 13** 5'-GATTTGCATA*TT*CATGAG.[13] Restricting the complementary strand generated a constrained loop on the modified strand (Table 5, bulges made with **ODN 13** and **ODN 15** to **20**) whereas expanding the complementary strand with unpaired moiety from one to six nucleotides led to bulged structures facing the constraint (Table 6, bulges made with **ODN 13** and **ODN 21** to **26**).

Phosphoramidites **7** and **15** were incorporated with similar yields than those obtained for unmodified nucleotide phosphoramidite with no change either in concentration nor in synthetic cycle time during automated oligonucleotide synthesis. An important point that need to be outlined was that the oxaza-phosphorinane structure of α,β-C_2NA was stable towards the ammonia treatment and even to the use of ammonia/methyl amine (AMA) at 65°C, with no detectable ODN degradation by ring opening, an issue encountered with their dioxa-phosphorinane-CNA analogues during synthesis of chimeric antisens oligonucleotides.[28] All the modified oligonucleotides were characterized by mass spectroscopy in MALDI Tof mode and showed an increased mass of 64 Da with respect to their unmodified analogues.

According to the preorganization concept, α,β-C_2NA featuring the B-DNA canonical α *gauche(-)* constraint induced a neat thermal stabilization of duplex with Δ*T*m around +3°C (±1°C) independently of the composition (**ODN 2** and **ODN 4**, Table 4) and the location (**ODN 4** compared to **ODN 5** and **6**, Table 4) of the constraint within the sequence. Despite this interesting impact on the duplex stability, the effect of α,β-C_2NA was lowered compared with the one exhibited by its α,β-D-CNA analogues (+5°C).[25] According to the *in silico* study in the ($R_{C5'}$, R_P) α,β-C_2NA, the appended hydrophobic propargyl substituent should be oriented towards the solvent and therefore could provide unfavourable interactions affecting the overall duplex stability.

Table 4. Sequences and thermal melting temperatures [°C] of ($R_{C5'}$, R_P) α,β-C_2NA TT featuring B-type canonical value (α = *gauche*(-), β = *trans*) containing duplexes and of ($S_{C5'}$, S_P) α,β-C_2NA TT featuring non-canonical value (α = *gauche*(+), β = *trans*) containing duplexes and hairpins.

ODN	Sequences[a]	*T*m[b]	Δ*T*m
1	5'-GCGCTTGCCG 3'-CGCGAACGGC	57.0	-
2	5'-GCGCTTGCCG 3'- CGCGAACGGC	60.0	+3.0
3	5'-GCGTTTTTGCT 3'-CGCAAAAAACGA	51.0	-
4	5'-GCGTTTTTGCT 3'-CGCAAAAAACGA	55.0	+4.0
5	5'-GCGTTTTTGCT 3'-CGCAAAAAACGA	54.0	+3.0
6	5'-GCGTTTTTGCT 3'-CGCAAAAAACGA	54.0	+3.0
7	5'-GCGCTTGCCG 3'- CGCGAACGGC	48.0	-9.0
8	5'-ATCCTA*TTTT*TAGGAT	52.0	-
9	5'-ATCCTA*TTT*TTAGGAT	50.0	-2.0
10	5'-ATCCTA*TT*TTAGGAT	58.0	+6.0
11	5'-ATCCTA*TTT*TAGGAT	54.0	+4.0
12	5'-ATCCTA*TT*TTAGGAT	53.0	+1.0

[a] TT = ($R_{C5'}$, R_P) α,β- C_2NA TT (g^-,t) or TT = ($S_{C5'}$, S_P) α,β- C_2NA TT (g^+,t) within the strand. T in italic indicates an unpaired thymidine within the structure [b] UV melting experiments were carried out in sodium phosphate buffer (10 mM, pH 7.0) containing NaCl (100 mM) and EDTA (1 mM). Melting temperatures (Tm) were measured as the maximum of the first derivate of the UV melting curve (OD260 vs temperature, 20-90 °C, 0.5 °C/min) which was recorded at concentration of 5 µM in sodium phosphate buffer (10 mM, pH 7.0) containing NaCl (100 mM) and EDTA (1 mM).

The *T*m measured for **ODN 7** (Table 4) and **ODN 14** (Table 5) showed that the *gauche(+)* constraint imposed by ($S_{C5'}$, S_P) α,β-C_2NA destabilized the duplex by -9°C and -7°C, respectively which reached the same level displayed by the corresponding α,β-D-CNA for the former. It confirmed that in this configuration there was again an additive negative effect brought by the propargyl function that should be oriented towards the minor groove of the duplex structure.

On the other hand, aside from the introduction of the constrain at the junction between the loop and the stem (**ODN 9**, Table 4) that appeared to be badly accommodated (Δ*T*m = -2°C), an improved thermal stability was depicted for ($S_{C5'}$, S_P) α,β-C_2NA modified hairpins (**ODN 10**, **11** and **12**, Table 4) that reached up to +6°C when the α *gauche(+)* constraint was located at the described turning phosphate position (**ODN 10**) and was superior to that induced by the α,β-D-CNA analogue. It can be proposed that the four thymidines composing the loop provided a favourable surrounding for the hydrophobic propargyl arm that could participate to π stacking and therefore improved the overall structure thermal stability.

Table 5. Thermal melting temperatures [°C] of bulges constructed with (GATTTGCATA*TT*CATGAG) where *TT*= α,β-C_2NA featuring (g^+,t) conformation is within the loop.

ODN	Target sequence 3'→5'	*T*m(Δ*T*m)[a] 5'-GATTTGCATA*TT*CATGAG	
		^{wt}*TT*[b]	*α,β-C₂NA*
14	CTAAACGTATAAGTACTC	55.0	48.0 (-7.0)
15	CTAAACGTAT AGTACTC	47	45.0 (-2.0)
16	CTAAACGTAT GTACTC	42	42.0 (0.0)
17	CTAAACGTA GTACTC	39.0	39.0 (0.0)
18	CTAAACGTA TACTC	35.0	34.0 (-1.0)
19	CTAAACGT TACTC	27.0	26.0 (-1.0)
20	CTAAACG TACTC	<25	26.0 (+1.0)

[a] Melting temperatures were measured as the maximum of the first derivate of the UV melting curve (OD260 vs temperature, 20-90 °C, 0.5 °C/min) which was recorded at concentration of 5 µM in sodium phosphate buffer (10 mM, pH 7.0) containing NaCl (100 mM) and EDTA (1 mM). [b] wt: unmodified phosphodiester internucleotidic linkage.

When inserted within bulged structures, ($S_{C5'}$, S_P) α,β-C_2NA exhibited two different behaviours (Tables 5 and 6).

When the *gauche(+)* constraint was installed within the loop it slightly destabilized the bulge (**ODN 15**, **18**, and **19**, Table 5) or can have no effect (**ODN 16** and **17**, Table 5) for loop size varying from one to five nucleotides. Only the rather unstable 6-nucleotides looped bulge made with **ODN 20** exhibited a small stability improvement. In that context, unlike its behaviour into T4-hairpin, the ($S_{C5'}$, S_P) α,β-C_2NA modification was not well tolerated and did not behave as its α,β-CNA analogue that improved, in the same conditions, the bulge thermal stabilities.[13]

In the other bulge construction, where the ($S_{C5'}$, S_P) α,β-C_2NA faced the growing loop (Table 6), it appeared that this modification conferred to the structures roughly the same thermal stability around 40 ±2°C regardless to the loop size. While for the one to three nucleotides loop the *gauche(+)* constraint was unfavourable or neutral (Table 6, bulges made with **ODN 21**, **22** or **23**), it turned out that it became stabilizing for loop made with at least four nucleotides (Table 6, bulges made with **ODN 24**, **25** or **26**) similarly to what has been observed with α,β-CNA analogues in the same context.[13]

Table 6. Thermal melting temperatures [°C] of bulges constructed with (GATTTGCATA*TT*CATGAG) where *TT*= α,β-C_2NA featuring (g^+,t) conformation is opposite to the loop.

ODN	Target sequence 3'→5'	*Tm*(Δ*Tm*)[a] 5'-GATTTGCATA*TT*CATGAG	
		^{wt}*TT*[b]	***α,β-C₂NA***
21	T CTAAACGTATA AGTACTC	48.0	44.0 (-4.0)
22	TC CTAAACGTATA AGTACTC	44.0	42.0 (-2.0)
23	TCT CTAAACGTATA AGTACTC	42.0	42.0 (0.0)
24	TCTC CTAAACGTATA AGTACTC	39	41.0 (+2.0)
25	TCTCT CTAAACGTATA AGTACTC	38	41.0 (+3.0)
26	TCTCTC CTAAACGTATA AGTACTC	36	38.0 (+2.0)

[a] Melting temperatures were measured as the maximum of the first derivate of the UV melting curve (OD260 vs temperature, 20-90°C, 0.5 °C/min) which was recorded at concentration of 5 µM in sodium phosphate buffer (10 mM, pH 7.0) containing NaCl (100 mM) and EDTA (1 mM). [b] wt: unmodified phosphodiester internucleotidic linkage

FAM decoration of α,β-C_2NA modified oligonucleotides

In order to validate the concept of constrained and convertible nucleotides, we had to show that α,β-C_2NA can be easily conjugated through the Huisgen's cycloaddition (CuAAC). We choose to decorate two ($R_{C5'}$, R_P) α,β-C_2NA modified ODN (**ODN 2** and **4** converted into **f-ODN 2** and **f-ODN 4**, respectively) and two ($S_{C5'}$, S_P) α,β-C_2NA modified ODN (**ODN 10** and **13** converted into **f-ODN 10** and **f-ODN 13**, respectively) with fluorescein by mean of its commercially available azide derivative (6-FAM-Azide, Figure 3).

Each conjugation proceeded cleanly in 1h in standard conditions (cat. $CuSO_4$, ascorbic acid) as indicated by reverse phase analytical HPLC monitoring. All the conjugates were characterized by mass spectroscopy in MALDI Tof mode and showed an increase of mass of 460 Da with respect to their precursors. Another common characteristic of the conjugates was depicted on the UV spectra where two maxima of absorption were observed at 260 and 497 nm that can be easily attributed to the nucleic bases for the former and to the fluorescein moiety for the latter. Therefore, the propargyl arm featured by α,β-C_2NA appeared to be a very good partner for CuAAC decoration of oligonucleotides.[28]

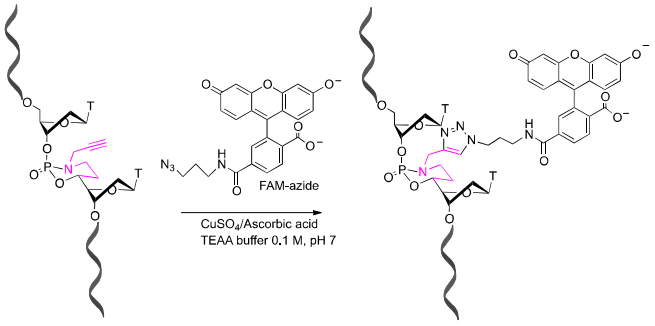

Fig. 3. : Conjugation with fluorescein of α,β-C_2NA modified ODN by CuAAC.

The thermal stability of the duplex made with conjugates were measured to get insight of the dye impact on the probe-target duplex when the conjugate was directed towards the solvent within **f-ODN 2** and **f-ODN 4** with a canonical α *gauche(-)* constraint or towards the minor groove within **f-ODN 13** with a non-canonical α *gauche(+)* constraint. Duplex formed with **f-ODN 2** and **f-ODN 4** and their respective complementary strand exhibited the same *Tm* value of 52°C and appeared to be less stable than those formed with their constrained precursor by -8 and -3°C, respectively. In the case of **f-ODN 2**, the *gauche(-)* constraint did not compensate the dye negative effect when compared with the corresponding unmodified **ODN 1** (Δ*T*m = -5°C) but with **f-ODN 4** the constraint restored the thermal stability to the level of the unmodified **ODN 3** (Δ*T*m = +1°C). Therefore, it looked like the *gauche(-)* constraint was able to compensate the negative effect on thermal stability induced by the dye depending on the sequence composition.

With a measured *Tm* of 44°C, combination of the *gauche(+)* constraint and the hydrophobic fluorescein were additive and decreased the *Tm* value of the duplex formed with **f-ODN 13** by -4°C relatively to its constrained precursor **ODN 13** and reached -11°C when compared to the wild type.

Interestingly, even if the conjugation was destabilizing (Δ*Tm* = -4°C) compared with **ODN 10,** hairpin structure **f-ODN 10** (*Tm* = 54°C) accommodated the dye decoration within the loop when compared with the unmodified hairpin **ODN 8** with a Δ*Tm* of +2°C and therefore ensure an overall stabilization of the highly modified structure.

Conclusions

In silico simulations showed us that the choice of dioxo-1,3,2-oxaza-phosphorinane structure with an appended propargyl function on the nitrogen atom for modifying the sugar/phosphate backbone within dinucleotide was perfectly adapted for the design of this new concept of convertible and constrained nucleic acid (C_2NA). The two major isomers *($R_{C5'}$, R_P)* and ($S_{C5'}$, S_P) α,β-C_2NA in which two torsional angle α an β are constrained within the cyclic system appeared to fit with a duplex or hairpin structure, respectively while keeping the propargyl arm accessible for further conjugation.

H-phosphonate chemistry provided a rapid access to the target compounds α,β-C_2NA starting from stereocontrolled 5'-C-propargylaminoethyl thymidine. The structural study by NMR means of ($R_{C5'}$, R_P) and ($S_{C5'}$, S_P) α,β-C_2NAs outlined that α and β were locked in *gauche(-)/trans* and *gauche(+)/trans* conformations, respectively. Accordingly with the calculation results and as expected for α torsional angle constrained into a B-type canonical conformation, incorporation of the ($R_{C5'}$, R_P) α,β-C_2NA isomer into oligonucleotides led to stabilization of DNA-duplex by an average increase of the melting temperature of +3°C.

On the other hand the ($S_{C5'}$, S_P) isomer featuring the non-canonical *gauche(+)* conformation of α, was poorly effective towards bulges structures but exhibited the highest level of hairpin structure thermal stability ever reached when installed within the loop moiety (ΔTm = +6°C).

As a proof of concept α,β-C_2NA constrained ODNs have been efficiently decorated with fluorescein through CuAAC and the thermal denaturation study showed that the benefit brought by the constraint when properly installed can compensate the destabilizing effect of the dye, generating ODNs with similar stability than unmodified ones but with enhanced properties.

These α,β-C_2NA represent the first elements of a new family of convertible and constrained nucleotides that will be extended to α,β,γ and δ,ε,ζ-C_2NA to have access to a large range of geometrical features. These neutral backbone-modified oligonucleotides could be used in lot of biological applications such as exon skipping, gene interference, antisense therapeutics applications and for the development of DNA based therapeutic agents relying on bioconjugation with increased stability and affinity for the target.[29]

Convertible and constrained nucleic acids should also found biotechnological applications such as SNP (Single Nucleotide Polymorphism) detection through fluorescence change upon hybridization, decoration and stabilisation of small branched DNA nanostructures and DNA origami staples modification for regio-controlled installation of new functionalities.[30]

Experimental

Compound 5'-C*(S)*-tosyloxyethyl-3'-*O*-*tert*-butyldiphenylsilyl-thymidine **1** and compound 5'-C*(R)*-tosyloxyethyl-3'-*O*-tert-butyldiphenylsilyl-thymidine **9** were prepared according procedures described in ref 14.

Compound **2**: 5'-C(S)-Propargylaminoethyl-3'-O-*tert*-butyldiphenylsilyl-thymidine.

To a solution of 5'-C*(S)*-tosyloxyethyl-thymidine **1** (500 mg, 0.74 mmol) in anhydrous acetonitrile (4 mL), were added ethyldi*iso*propylamine (1.28 mL, 7.4 mmol) and propargyl amine (0.473 mL, 7.4 mmol). After stirring at 45°C for 12h, the solvent and volatile reactants were removed under *vacuo*. The crude material was extracted with ethyl acetate and washed with a saturated aqueous solution of $NaHCO_3$ and brine. **2** (270 mg, 65%) was isolated after silica gel chromatography with ethyl acetate as solvent. ^{1}H NMR (300 MHz, $CDCl_3$): δ = 7.84 (d, 1H, *J* = 1.2 Hz, H_6), 7.64-7.60 (m, 4H, Ph), 7.42-7.36 (m, 6H, Ph), 6.47 (dd, 1H, *J* = 5.4 and 9.0 Hz, $H_{1'}$), 4.47 (dt, 1H, *J* = 1.5 and 5.7 Hz, H_3), 3.71 (t, 1H, *J* = 1.5 Hz, $H_{4'}$), 3.34 and 3.33 (AB part of an ABX syst, 2H, *J* = 2.4 and 16.8 Hz, $H_{8'}$), 3.30 (dt, 1H, *J* = 1.5 and 10 Hz, $H_{5'}$), 3.12 (dt, 1H, *J* = 3.8 and 12.3 Hz, $H_{7'}$), 2.58 (td, 1H, *J* = 2.7 and 12.3 Hz, $H_{7'}$), 2.20 (t, 1H, *J* = 2.4 Hz, $H_{9'}$), 2.19 (A part of an ABX syst, 1H, *J* = 1.5, 5.4 and 13.2 Hz, $H_{2'}$), 2.01 (B part of an ABX syst, 1H, *J* = 5.4, 8.4 and 13.2 Hz, $H_{2'}$), 1.82 (d, 3H, *J* = 1.2 Hz, Me), 1.63 (m, 1H, $H_{6'}$), 1.30 (m, 1H, $H_{6'}$), 1.06 (s, 9H, *t*Bu). ^{13}C NMR (75 MHz, $CDCl_3$): δ ppm = 164.1, 151.0, 141.3, 140.5, 137.3, 135.8, 133.4, 133.1, 130.1, 128.8, 127.9, 125.8, 111.0, 90.3, 86.6, 75.4, 74.9, 70.9, 45.9, 39.7, 37.0, 30.4, 26.9, 19.0, 12.5 ppm. HRMS (ESI):cald. 562.2737 for $C_{31}H_{40}N_3O_5Si$; found 562.2718.

Compound **3**: (S_P,$S_{C5'}$)-5'-*O*-Dimethoxytrityl-3'-*O*-*tert*-butylldiphenylsilyl-α,β-C_2NA TT and compound **4**: (R_P,$S_{C5'}$)-5'-*O*-Dimethoxytrityl-3'-*O*-*tert*-butylldiphenylsilyl-α,β-C_2NA TT.

To a solution of 5'-*O*-dimethoxy-tritylthymidine 3'-*H*-phosphonate (312 mg, 0.44 mmol, 1eq.) in anhydrous pyridine (3 mL) was added pivaloyl chloride (162 µL, 3eq). After 15 min this solution was transferred to a solution of **2** (247 mg, 0.44 mmol) in anhydrous pyridine (1.5 mL) at room temperature. After 30 min of stirring, a solution of iodine (0.02 M in THF/pyr/H_2O, 7:2:1) was added drop wise until a dark brown colour persists. The reaction medium was diluted with ethyl acetate and an aqueous solution of 10% of sodium thiosulfate was added until the brown colour disappeared. The organic layer was washed with brine and dried over magnesium sulphate and the solvent removed under vacuum. Compound **3** and **4** were separated by silica gel column chromatography eluting with a mixture of EtOAc/CH_2Cl_2 (2:3 to 4:1) and obtained as white foam in 80% yield (238 mg and 125 mg, respectively). Compound **3**: ^{1}H NMR (500 MHz, $CDCl_3$): δ ppm = 9.13 (m, 1H, NH), 8.76 (m, 1H, NH), 7.59-7.17 (m, 21H, Ph and H_6), 6.83-6.78 (m, 4H, Ph), 6.58 (dd, 1H, *J* = 5.0 and 9.5 Hz, $H_{1'b}$), 6.46 (dd, 1H, *J* = 10.0 and 5.5 Hz, $H_{1'a}$), 5.07 (t, 1H, *J* = 5.0 and $J_{H/P}$ = 8.0 Hz, $H_{3'a}$), 4.15 (d, 1H, *J* = 5.5 Hz, $H_{3'b}$), 3.94 (ddd, 1H, *J* = 2.5, 18.0 and $J_{H/P}$ = 9.0 Hz, $H_{8'b}$), 3.86 (bs, 1H, $H_{4'a}$), 3.77 and 3.76 (s, 6H, OMe), 3.70 (d, 1H, $J_{H/P}$ = 5.5 Hz, $H_{4'b}$), 3,63 (ddd, 1H, *J* = 2.5, 18.0 and $J_{H/P}$ = 16.5 Hz, $H_{8'b}$), 3.32 (bd, 1H, *J* = 11.5 and $J_{H/P}$ < 1 Hz, $H_{5'b}$), 3.27 (A part of an ABX syst, 1H, *J* = 2.0 and 10.5 Hz, $H_{5'a}$), 3.14 (B part of an ABX syst, 1H, *J* = 2.5 and 10.5 Hz, $H_{5'a}$), 3.12 (m, 1H, *J* = 3.0, 12.5 and $J_{H/P}$ < 1 Hz, $H_{7'b}$), 3.07 (m, 1H, *J* = 2.5, 5.0, 12.5 and $J_{H/P}$ = 24.0 Hz, $H_{7'b}$), 2.51 (A part of an ABX syst, 1H, *J* = 5.0 and 14.0 Hz, $H_{2'a}$), 2.37 (t, 1H, *J* = 2.5 Hz, $H_{10'b}$), 2.36 (m, 1H, *J* = 6.0 and 14.0 Hz, $H_{2'a}$), 2.20 (A part of an ABX syst, 1H, *J* = 5.0 and 12.5 Hz, $H_{2'b}$), 2.07 (m, 1H, $H_{6'b}$), 1.91 (d, 3H, *J* = 1.1 Hz, Me), 1.87 (B part of an ABX syst, 1H, *J* = 5.5, 9.0 and 12.5 Hz, $H_{2'b}$), 1.34 (d, 3H, *J* = 1.1 Hz, Me), 1.29 (m, 1H, $H_{6'b}$), 1.03 (s, 9H, *t*Bu). ^{13}C NMR (125 MHz, $CDCl_3$): δ ppm = 163.7, 163.6, 158.9, 158.8, 150.7, 150.6, 144.0, 135.8, 135.7, 135.5, 135.4, 135.0, 134.9, 133.2, 132.4, 130.5, 130.3, 130.2, 130.1, 128.2, 128.1, 128.0, 127.9, 127.4, 113.4, 112.1, 111.9, 85.2, 84.9, 84.5, 80.1, 78.5, 78.3, 75.1, 73.8, 63.5, 55.3, 45.7, 39.9, 39.4, 37.8, 29.7, 27.4, 26.9, 19.0, 12.4, 11.6. ^{31}P NMR (202 MHz, $CDCl_3$): δ = 2.4 ppm.

HRMS (ESI): cald. 1172.4218 for $C_{62}H_{68}N_5O_{13}PSiNa$; found 1172.4219.

Compound **4**: ^{1}H NMR (500 MHz, $CDCl_3$): δ ppm = 9.00 (m, 1H, NH), 8.94 (m, 1H, NH), 7.65-7.58 (m, 4H, Ph), 7.47 (bd, 1H, *J* = 1.1 Hz, H_6), 7.45-7.19 (m, 15H, Ph), 7.10 (bd, 1H, *J* = 1.1 Hz, H_6), 6.81-6.79 (m, 4H, Ph), 6.39 (dd, 1H, *J* = 6.0 and 8.0 Hz, $H_{1'b}$), 6.28 (dd, 1H, *J* = 6.0 and 8.0 Hz, $H_{1'a}$), 5.04 (m, 1H, $J_{H/P}$ = 7.2 Hz, $H_{3'a}$), 4.44 (m, 1H, $H_{3'b}$), 4.07 (bd, 1H, *J* = 2.5 Hz, $H_{4'a}$), 3.89 (ddd, 1H, *J* = 2.5, 18.0 Hz and $J_{H/P}$ = 9.5 Hz, $H_{8'b}$), 3.76 (s, 6H, OMe), 3.69 (q, 1H, *J* = 2.5, 2.5 Hz and $J_{H/P}$ = 4.0 Hz, $H_{4'b}$), 3.56 (dt, 1H, *J* = 1.8, 10.5 Hz and $J_{H/P}$ = 2.0 Hz, $H_{5'b}$), 3.52 (ddd, 1H, *J* = 2.5, 18.0 Hz and $J_{H/P}$ = 11.5 Hz, $H_{8'b}$), 3.51 and 3.32 (AB part of an ABX syst, 2H, *J* = 2.5, 2.5 and 1.0 Hz, $H_{5'a}$), 3.10 (m, 1H, *J* = 3.0, 12.5 Hz and $J_{H/P}$ = 8.5 Hz, $H_{7'b}$), 2.86 (m, 1H, *J* = 2.5, 5.0, 12.5 Hz and $J_{H/P}$ = 12.0 Hz, $H_{7'b}$), 2.47 (A part of an ABX syst, 1H, *J* = 2.0, 8.0 and 14.0 Hz, $H_{2'a}$), 2.34 (m, 1H, *J* = 2.5, 6.0 and 13.5 Hz, $H_{2'a}$), 2.32 (m, 1H, $H_{2'b}$), 1.99 (t, 1H, *J* = 2.3 Hz, $H_{10'b}$), 1.90 (m, 1H, $H_{6'b}$), 1.83 (d, 3H, *J* = 1.1 Hz, Me), 1.80 (m, 1H, $H_{2'b}$), 1.52 (m, 1H, $H_{6'b}$), 1.31 (d, 3H, *J* = 1.1 Hz, Me), 1.06 (s, 9H, *t*Bu). ^{13}C NMR (125 MHz, $CDCl_3$): δ ppm = 163.7, 163.6, 158.9, 158.8, 150.4, 150.2, 144.0, 135.9, 135.8, 135.7, 135.3, 135.2, 135.1, 135.0, 133.3, 132.6, 130.2, 130.1, 128.3, 128.1, 127.3, 113.3, 111.5, 111.4, 84.6, 84.4, 84.3, 77.7, 77.6, 73.2, 73.0, 63.3, 55.3, 44.6, 40.1, 39.2, 37.7, 27.1, 26.9, 19.0, 12.8, 11.6. ^{31}P NMR (202 MHz, $CDCl_3$): δ = 4.67 ppm. HRMS (ESI): cald. 1172.4218 for $C_{62}H_{68}N_5O_{13}PSiNa$; found 1172.4244.

Compound **5**: (S_P,$S_{C5'}$)-5'-*O*-Dimethoxytrityl-α,β-C_2NA TT.
To a solution of compound **3** (300 mg, 0.26 mmol) in anhydrous THF (4 mL) was added at room temperature nBu_4NF (1 M sol in THF, 300 µL, 0.3 mmol, 1.15 eq.). After 1h of stirring the reaction medium was concentrated under vacuum and submitted to silica gel column chromatography eluting with ethyl acetate. Compound **5** was isolated as a white foam in 85% yield (200 mg). Probably due to the formation of aggregates in solution, the NMR spectra were recorded with a very poor resolution for ^{1}H and with a lack of detection of several aliphatic carbon for ^{13}C. This phenomenon has already been observed for α,β-D-CNA (see supporting information of Le Clézio *et al*. *Org. Lett*. **2003**, *5*, 161-164, ref 16).
^{1}H NMR (300 MHz, $CDCl_3$): δ ppm = 9.52 (m, 1H, NH), 9.19 (m, 1H, NH), 7.52 (bd, 1H, *J* = 1.2 Hz, H_6), 7.47 (bd, 1H, *J* = 1.2 Hz, H_6), 7.35-7.21 (m, 9H, Ph), 6.82-6.79 (m, 4H, Ph), 6.46 (dd, 1H, *J* = 5.4 and 8.4 Hz, $H_{1'}$), 6.39 (t, 1H, *J* = 6.6 Hz, $H_{1'}$), 5.09 (bt, 1H, *J* = 6.2 Hz, $H_{3'a}$), 4.51 (bd, 1H, *J* = 11.0 Hz), 4.32-4.27 (m, 2H), 4.02 (ddd, 1H, *J* = 2.1, 7.8 and 17.4 Hz, $H_{8'}$), 3.87 (m, 1H), 3.76 (s, 6H, OMe), 3.72-3.64 (m, 2H), 3.52-3.32 (m, 4H), 3.16 (m, 1H, $H_{8'}$), 2.58 (A part of an ABX syst, 1H, *J* = 5.1 and 13.8 Hz, $H_{2'}$), 2.46 (m, 1H), 2.36 (t, 1H, *J* = 2.3 Hz, $H_{10'}$), 2.29-2.05 (m, 3H), 1.91 (s, 3H, Me), 1.70 (m, 1H), 1.39 (s, 3H, Me). ^{13}C NMR (75 MHz, $CDCl_3$): δ ppm = 164.4, 164.2, 158.9, 151.3, 151.1, 144.2, 135.6, 135.2, 130.3, 128.2, 127.4, 113.6, 112.2, 112.0, 85.0, 84.9, 84.7, 78.4, 73.9, 72.4, 68.1, 67.2, 63.9, 55.4, 38.0, 37.9, 29.8, 12.6, 11.8. ^{31}P NMR (121 MHz, $CDCl_3$): δ = 2.7 ppm. HRMS (ESI): cald. 934.3040 for $C_{46}H_{50}N_5O_{13}PNa$; found 934.3037.

Compound **6**: (R_P,$S_{C5'}$)-5'-*O*-Dimethoxytrityl-α,β-C_2NA TT.
Compound **6** (110 mg, 0.12 mmol) was obtained as a white foam in 90% yield from **4** (153 mg, 0.13 mmol) by the same procedure as described for **5** and the same problem in NMR analysis was encountered. ^{1}H NMR (300 MHz, $CDCl_3$): δ ppm = 9.83 (bs, 2H, NH), 7.53 (bs, 1H, H_6), 7.34-7.20 (m, 10H, Ph), 6.81 (d, 2H, Ph); 6.33 (dd, 1H, *J* = 5.1 and 8.7 Hz, $H_{1'}$), 6.24 (t, 1H, *J* = 6.9 Hz, $H_{1'}$), 5.15 (bt, 1H, *J* = 4.8 Hz, $H_{3'a}$), 4.61 (m, 1H), 4.47 (m, 1H), 4.19 (s, 1H), 3.94 (m, 1H), 3.88 (m, 1H), 3.75 (s, 6H, OMe), 3.60 (m, 1H), 3.46 (m, 1H), 3.34-3.17 (m, 3H), 2.65 (A part of an ABX syst, 1H, *J* = 5.7 and 13.5 Hz, $H_{2'}$), 2.37 (m, 2H), 2.20 (m, 2H), 2.08 (t, 1H, *J* = 2.3 Hz, $H_{10'}$), 1.95 (m, 1H), 1.86 (s, 3H, Me), 1.30 (s, 3H, Me), 1.22 (m, 1H). ^{13}C NMR (75 MHz, $CDCl_3$): δ ppm = 164.2, 158.7, 150.9, 144.0, 135.0, 130.2, 128.2, 128.1, 113.4, 111.7, 111.3, 86.3, 85.1, 84.6, 84.4, 78.8, 73.1, 70.8, 68.1, 63.5, 55.3, 45.0, 39.9, 37.6, 29.7, 12.7, 11.7. ^{31}P NMR (121 MHz, $CDCl_3$): δ = 4.5 ppm. HRMS (ESI): cald. 934.3040 for $C_{46}H_{50}N_5O_{13}PNa$; found 934.3030.

Compound **7**: (S_P,$S_{C5'}$)-5'-*O*-Dimethoxytrityl-3'-*O*-(cyanoethyl-diisopropylamino-phosphoramidite)-α,β-C_2NA TT.
Compound **5** (215 mg, 0.23 mmol) was dissolved under argon in dry THF (2 mL) at room temperature. *N*-Ethyldi*iso*propylamine (0.164 mL, 0.94 mmol) and then 2-cyanoethyl-*N*,*N*-di*iso*propylchlorophosphoramidite (111 mg, 0.471 mmol) were added. The reaction mixture was stirred for 2h, the white precipitate was filtered and the filtrate diluted in EtOAc saturated with argon. The organic layer was washed with a cold aqueous solution of potassium carbonate (10%), dried over $MgSO_4$, filtered and concentrated with care under reduced pressure. The crude was then purified by silica gel column chromatography eluting with a mixture of EtOAc/Et_3N (10:0.02) to give **7** (95%, 248 mg) contaminated with inseparable small amount of residual *H*-phosphonate as a white foam. Because the α,β-C_2NA TT phosphoramidites are isolated as a mixture of diastereomers, the ^{1}H and ^{13}C NMR spectra were highly complicated and therefore are not presented even if some characteristic signals can be recognized. ^{31}P NMR (121 MHz, $CDCl_3$): δ = 150.1, 147.7, 3.1, 2.7 ppm. HRMS (ESI): cald. 1134.4119 for $C_{55}H_{68}N_7O_{14}P_2Na$; found 1134.4139.

Compound **8**: (R_P,$S_{C5'}$)-5'-*O*-Dimethoxytrityl-3'-*O*-(cyanoethyl-diisopropylamino-phosphoramidite)-α,β-C_2NA TT.
Compound **8** (150 mg, 0.135 mmol) was obtained as a white foam in 87% yield from **6** (142 mg, 0.155 mmol) by the same procedure as described for **7** and the same problem in NMR analysis was encountered. ^{31}P NMR (121 MHz, $CDCl_3$): δ = 149.6, 148.6, 4.9, 4.5 ppm. HRMS (ESI): cald. 1112.4299 for $C_{55}H_{68}N_7O_{14}P_2$; found 1112. 4326.

Compound **10**: 5'-C(*R*)-Propargylaminoethyl-3'-*O*-*tert*-butyldiphenylsilyl-thymidine.
To a solution of tosyloxyethyl-thymidine **9** (934 mg, 1.37 mmol) in anhydrous dimethylformamide (6 mL), were added ethyldi*iso*propyl amine (1.20 mL, 6.85 mmol) and propargyl amine (0.881 mL, 13.7 mmol). After stirring at 30°C for 24h, the solvent and volatile reactants were removed under *vacuo*. The

crude material was extracted with ethyl acetate and washed with a 10% aqueous solution of Na_2CO_3 and brine. **10** (762 mg, quant) was isolated after silica gel chromatography with ethyl acetate/methanol (95:5) as solvent. ^{1}H NMR (300 MHz, $CDCl_3$): δ = 7.75 (d, 1H, *J* = 1.2 Hz, H_6), 7.68-7.63 (m, 4H, Ph), 7.44-7.35 (m, 6H, Ph), 6.48 (dd, 1H, *J* = 5.4 and 9.1 Hz, $H_{1'}$), 4.45 (bd, 1H, *J* = 4.8 Hz, $H_{3'}$), 3.85-3.80 (m, 2H, $H_{5'}$ and $H_{4'}$), 3.26 (d, 2H, *J* = 2.3 Hz, $H_{8'}$), 3.12 (dt, 1H, *J* = 3.7 and 12.4 Hz, $H_{7'}$), 2.56 (td, 1H, *J* = 2.8 and 11.9 Hz, $H_{7'}$), 2.21 (m, 1H, $H_{2'}$), 2.20 (t, 1H, *J* = 2.4 Hz, $H_{10'}$), 2.02 (B part of an ABX syst, 1H, *J* = 5.0, 9.0 and 14.2 Hz, $H_{2'}$), 1.85 (d, 3H, *J* = 1.2 Hz, Me), 1.06 (s, 9H, *t*Bu), 1.02 (m, 1H, $H_{6'}$), 0.76 (m, 1H, $H_{6'}$). ^{13}C NMR (75 MHz, $CDCl_3$): δ ppm = 164.4, 150.9, 136.9, 136.1, 136.0, 133.4, 130.1, 127.9, 111.0, 91.3, 85.2, 81.0, 77.9, 73.4, 47.1, 41.1, 37.4, 29.9, 27.0, 19.2, 12.7. HRMS (ESI): cald. 562.2737 for $C_{31}H_{40}N_3O_5Si$; found 562.2727.

Compound **11**: (R_P,$R_{C5'}$)-5'-*O*-Dimethoxytrityl-3'-*O*-*tert*-butyldiphenylsilyl-α,β-C_2NA TT and compound **12**: (S_P,$R_{C5'}$)-5'-*O*-Dimethoxytrityl-3'-*O*-*tert*-butyldiphenylsilyl-α,β-C_2NA TT.
Starting from **10** (526 mg, 0.937 mmol) and following the procedure described for α,β-C_2NA TT **3** and **4**, compound **11** and **12** were isolated as white foam in 60% overall yield (592 mg and 50 mg, respectively). Whereas the diastereoisomeric ratio measured by ^{31}P NMR on the crude was 3:1 in favour of **11**, it appeared that **12** was sensitive to the chromatographic conditions and partially decomposed. Compound **11**: ^{1}H NMR (500 MHz, $CDCl_3$): δ ppm = 9.16 (m, 1H, NH), 9.08 (m, 1H, NH), 7.67-7.18 (m, 21H, Ph and H_6), 6.83-6.79 (m, 4H, Ph), 6.40 (dd, 1H, *J* = 6.0 and 8.7 Hz, $H_{1'b}$), 6.34 (dd, 1H, *J* = 5.4 and 8.7 Hz, $H_{1'a}$), 5.07 (t, 1H, *J* = 4.8 and $J_{H/P}$ = 6.9 Hz, $H_{3'a}$), 4.53 (d, 1H, *J* = 5.4 Hz, $H_{3'b}$), 4.32 (m, 1H, *J* = 11.7, 4.0, 3.0 and $J_{H/P}$ < 1 Hz, $H_{5'b}$), 4.19 (bs, 1H, $H_{4'a}$), 3.96 (m, 1H, *J* = 3.9, 4.0, and $J_{H/P}$ = 3.6 Hz, $H_{4'b}$), 3.84 (ddd, 1H, *J* = 2.5, 18.0 and $J_{H/P}$ = 7.5 Hz, $H_{8'b}$), 3.77 (s, 6H, OMe), 3,56 (ddd, 1H, *J* = 2.4, 18.0 and $J_{H/P}$ = 17.7 Hz, $H_{8'b}$), 3.15 (A part of an ABX syst, 1H, *J* = 2.4 and 10.5 Hz, $H_{5'a}$), 3.34 (B part of an ABX syst, 1H, *J* = 2.7 and 10.5 Hz, $H_{5'a}$), 3.15 (m, 1H, *J* = 3.6, 12.3 and $J_{H/P}$ < 1 Hz, $H_{7'b}$), 2.87 (m, 1H, $J_{H/P}$ = 22.0 Hz, $H_{7'b}$), 2.29 (A part of an ABX syst, 1H, *J* = 2.0, 4.8 and 14.1 Hz, $H_{2'a}$), 2.19 (m, 1H, $H_{2'a}$), 2.14 (m, 1H, $H_{2'b}$), 2.05 (t, 1H, *J* = 2.4 Hz, $H_{10'b}$), 2.03 (m, 1H, $H_{2'b}$), 1.81 (d, 3H, *J* = 1.1 Hz, Me), 1.42 (m, 1H, $H_{6'b}$), 1.34 (m, 1H, $H_{6'b}$), 1.29 (d, 3H, *J* = 1.1 Hz, Me), 1.05 (s, 9H, tBu). ^{13}C NMR (125 MHz, $CDCl_3$): δ = 164.1, 163.9, 158.8, 150.9, 150.8, 144.0, 136.0, 135.8, 35.0, 132.9, 132.8, 130.1, 128.3, 128.0, 113.4, 111,8, 111.3, 88.2, 88.0, 87.3, 84.7, 84.6, 84.2, 80.3, 80.2, 78.2, 77.7, 73.3, 72.6, 63.4, 55.3, 46.1, 39.7, 38.6, 37.6, 29.7, 26.9, 19.1, 12.6, 11.6. ^{31}P NMR (202 MHz, $CDCl_3$): δ = 2.7 ppm. HRMS (ESI): cald. 1172.4218 for $C_{62}H_{68}N_5O_{13}PSiNa$; found 1172.4210.

Compound **12**: ^{1}H NMR (500 MHz, $CDCl_3$): δ ppm = 8.99 (m, 1H, NH), 8.72 (m, 1H, NH), 7.68-7.21 (m, 21H, Ph and H_6), 6.85-6.81 (m, 4H, Ph), 6.40 (dd, 1H, *J* = 5.4 and 9.3 Hz, $H_{1'b}$), 6.35 (dd, 1H, *J* = 5.7 and 9.3 Hz, $H_{1'a}$), 5.03 (t, 1H, *J* = 5.1 and $J_{H/P}$ = 7.5 Hz, $H_{3'a}$), 4.36 (d, 1H, *J* = 5.1 Hz, $H_{3'b}$), 4.30 (m, 1H, *J* = 11.1, 2.7, 2.7 Hz and $J_{H/P}$ = 2.1 Hz, $H_{5'b}$), 4.06 (ddd, 1H, *J* = 2.7, 18.0 and $J_{H/P}$ = 8.1 Hz, $H_{8'b}$), 3.94 (bs, 1H, $H_{4'a}$), 3.90 (bt, 1H, *J* = 1.8 and $J_{H/P}$ = 5.4 Hz, $H_{4'b}$), 3.80 (s, 6H, OMe), 3.57 (ddd, 1H, *J* = 2.4, 18.0 and $J_{H/P}$ = 15.3 Hz, $H_{8'b}$), 3.34 (A part of an ABX syst, 1H, *J* = 1.8 and 10.8 Hz, $H_{5'a}$), 3.17 (B part of an ABX syst, 1H, *J* = 2.4 and 10.8 Hz, $H_{5'a}$), 3.14 (m, 1H, $H_{7'b}$), 2.93 (m, 1H, $J_{H/P}$ = 15.0 Hz, $H_{7'b}$), 2.48 (A part of an ABX syst, 1H, *J* = 5.4 and 14.0 Hz, $H_{2'a}$), 2.36 (t, 1H, *J* = 2.3 Hz, $H_{10'b}$), 2.33 (m, 1H, $H_{2'a}$), 2.14 (m, 1H, $H_{2'b}$), 1.80 (m, 1H, $H_{2'b}$), 1.88 (d, 3H, *J* = 1.1 Hz, Me), 1.37-1.22 (m, 2H, $H_{6'b}$), 1.34 (d, 3H, *J* = 1.1 Hz, Me), 1.02 (s, 9H, *t*Bu). ^{13}C NMR (125 MHz, $CDCl_3$): δ = 164.0, 163.9, 159.0, 150.8, 150.5, 144.1, 136.0, 135.9, 135.2, 135.1, 132.9, 132.8, 130.5, 130.4, 130.2, 128.4, 128.3, 128.2, 113.5, 111.9, 88.6, 88.5, 87.4, 85.5, 85.3, 85.1, 84.6, 79.9, 79.8, 78.6, 73.8, 73.1, 67.2, 63.7, 54.4, 44.7, 40.2, 37.6, 31.1, 27.0, 19.3, 12.7, 11.7. ^{31}P NMR (202 MHz, $CDCl_3$): δ = 3.2 ppm. HRMS (ESI): cald. 1172.4218 for $C_{62}H_{68}N_5O_{13}PSiNa$; found 1172.4219.

Compound **13**: (R_P,$R_{C5'}$)-5'-*O*-Dimethoxytrityl-α,β-C_2NA TT
Compound **13** (310 mg, 0.34 mmol) was obtained as a white foam in 87% yield from **11** (450 mg, 0.39 mmol) by the same procedure as described for **5** and the same problem in NMR analysis was encountered. ^{1}H NMR (300 MHz, $CDCl_3$): δ ppm = 7.55 (ds, 1H, H_6), 7.34-7.20 (m, 10H, H_6 and Ph), 6.80 (d, 4H, Ph), 6.44 (dd, 1H, *J* = 5.1 and 9.6 Hz, $H_{1'}$), 6.27 (dd, 1H, *J*= 6.3 and 8.1 Hz, $H_{1'}$), 5.08 (bt, 1H, *J* = 4.2 and $J_{H/P}$ = 6.7 Hz, $H_{3'a}$), 4.65-4.58 (m, 2H), 4.38 (bs, 1H), 4.12 (ddd, 1H, *J* = 2.4, 17.7 and $J_{H/P}$ = 9.0 Hz, $H_{8'b}$), 3.94 (m, 1H), 3.76 (s, 6H, OMe), 3.72 (m, H), 3.63 (ddd, 1H, *J* = 2.4, 17.7 and $J_{H/P}$ = 13.5 Hz, $H_{8'b}$), 3.43 (m, 3H), 3.26-3.15 (m, 1H), 2.55-2.31 (m, 3H, $H_{2'}$), 2.25-2.08 (m, 3H), 2.21 (t, 1H, *J* = 2.4 Hz, $H_{10'b}$), 1.83 (d, 3H, *J* = 1.2 Hz, Me), 1.36 (d, 3H, *J* = 1.2 Hz, Me). ^{13}C NMR (75 MHz, $CDCl_3$): δ ppm = 164.1, 163.9, 158.8, 151.4, 150.6, 144.2, 135.2, 135.1, 130.1, 128.3, 128.2, 127.5, 113.4, 112.2, 111.6, 87.3, 85.4, 84.9, 84.5, 73.2, 70.5, 67.9, 67.0, 63.7, 55.3, 40.2, 39.1, 37.7, 26.4, 12.6, 11.7. ^{31}P NMR (121 MHz, $CDCl_3$): δ = 2.2 ppm. HRMS (ESI): cald. 934.3040 for $C_{46}H_{50}N_5O_{13}PNa$; found 934.3030.

Compound **14**: (S_P,$R_{C5'}$)-5'-*O*-Dimethoxytrityl-α,β-C_2NA TT.
Compound **14** (34 mg, 0.037 mmol) was obtained as a white foam in 85% yield from **12** (50 mg, 0.044 mmol) by the same procedure as described for **5** and the same problem in NMR analysis was encountered. ^{1}H NMR (300 MHz, $CDCl_3$): δ ppm = 7.47 (s, 1H, H_6), 7.33-7.17 (m, 10H, H_6 and Ph), 6.79 (d, 4H, Ph), 6.35 (t, 1H, *J* = 6.7 Hz, $H_{1'}$), 6.24 (t, 1H, *J* = 6.6 Hz, $H_{1'}$), 5.14 (m, 1H, $H_{3'a}$), 4.59 (m, 2H), 4.21 (bs, 1H), 3.90-3.83 (m, 2H), 3.73 (s, 6H, OMe), 3.68-3.24 (m, 6H), 3.13-3.01 (m, 2H), 2.58 (m, 1H, $H_{2'}$), 2.28 (m, 3H), 1.86 (m, 1H), 1.80 (s, 3H, Me), 1.28 (s, 3H, Me). ^{13}C NMR (75 MHz, $CDCl_3$): δ ppm = 164.2, 158.9, 151.1, 144.2, 136.5, 135.2, 130.3, 128.3, 128.2, 127.4, 113.5, 112.0, 111.4, 87.4, 87.2, 85.1, 84.9, 84.8, 84.5, 80.5, 80.4, 78.2, 73.4, 70.5, 63.6, 55.4, 46.4, 39.6, 38.9, 37.7, 27.7, 12.7, 11.8. ^{31}P NMR (121 MHz, $CDCl_3$): δ = 3.2 ppm. HRMS (ESI): cald. 934.3040 for $C_{46}H_{50}N_5O_{13}PNa$; found 934.3036.

Compound **15**: (R_P,$R_{C5'}$)-5'-*O*-Dimethoxytrityl-3'-*O*-(cyanoethyl-diisopropylamino-phosphoramidite)-α,β-C_2NA TT.
Compound **15** (454 mg, 0.37 mmol) was obtained as a white foam in 94% yield from **13** (397 mg, 0.44 mmol) by the same procedure as described for **7** and the same problem in NMR

analysis was encountered. ^{31}P NMR (121 MHz, $CDCl_3$): δ = 149.7, 148.9, 2.85, 2.83 ppm. HRMS (ESI): cald. 1112.4299 for $C_{55}H_{68}N_7O_{14}P_2$; found 1112.4304.

Compound **16**: (S_P,$R_{C5'}$)-5'-*O*-Dimethoxytrityl-3'-O-(cyanoethyl-diisopropylamino-phosphoramidite)-α,β-C_2NA TT.
Compound **16** (29 mg, 0.027 mmol) was obtained as a white foam in 72% yield from **14** (34 mg, 0.037 mmol) by the same procedure as described for **7** and the same problem in NMR analysis encountered. ^{31}P NMR (121 MHz, $CDCl_3$): δ = 149.1, 148.7, 3.7, 3.3 ppm. HRMS (ESI): cald. 1112.4299 for $C_{55}H_{68}N_7O_{14}P_2$; found 1112.4302.

Computational details

To investigate the dinucleotides conformation space, Langevin dynamics were performed (with a damping coefficient set to 2 ps^{-1}) using the Vienna Ab initio Simulation Package VASP.[31] In the VASP scheme, pseudo-potentials within the projector augmented wave method were employed together[32] with one of the dispersion-corrected functionals implemented in the VASP package, namely optB86b-vdw (dispersion correction is missing in conventional DFT functionals).[33] The wave function was expanded on a plane-waves basis set up to a kinetic energy cut-off of 300 eV and the simulation box size was large enough to avoid any interaction between the dinucleotide and its periodic images. A k-point sampling restricted to a single Γ-point was sufficient to ensure the good convergence of the total energy. This method was chosen to explore the conformation space because of its high computationally efficiency. All subsequent geometry optimizations were performed using the Gaussian 09 set of programs.[34] The Grimme's B97-D DFT functional[35], which includes an explicit dispersion correction term, was used together with the Def2-TZVP basis set. This combination was chosen for the minimization step of the dinucleotides on the basis of a benchmark covering thermochemistry, kinetics and non-covalent interactions.[36] Structural parameters result from full geometry optimization in the gas phase, with no imposed constraints, and default SCF and geometry optimization criteria were used. Vibrational frequencies were calculated in order to verify that the localized stationary points coincide with energy minima. The partial charges were calculated using the Natural Bond Orbital method (NBO) implemented in the Gaussian 09 program.

Oligonucleotides synthesis

The oligonucleotides were assembled on polystyrene support (0.2 μmol scale) on a ABI 394 using the standard phosphoramidite chemistry. After complete assembly of the oligonucleotide chain, deprotection was achieved with NH_4OH (33%) at 25°C for 24 h or with AMA 10 min at 65°C. The crude product was analysed and purified by reversed phase HPLC (Waters X Bridge OST C_{18}, 2.5 μm, 50 x 4.6 mm for analysis or 50 x 10 mm for purification scale) on Waters apparatus (Alliance system and a 996 photodiode array detector), using a gradient from 95% of A to 85% of A in B (A: TEAA buffer 0.05 M, pH 7.0; B: CH_3CN). Analyses of the oligonucleotides were performed by mass spectrometry in MALDI TOF mode on a PerSeptive Biosystems Voyager Spectrometer with THAP, 10% ammonium citrate as matrix.

Thermal denaturation studies

Absorbance versus temperature profiles were recorded at 260 nm in fused quartz cuvettes on a Carry 300 Bio spectrophotometer equipped with a Peltier temperature control device. Each sample was heated to 90°C and then slowly cooled before measurements. The temperature is increased by 0.5°C/min from 15 to 90°C. The two complementary strands were in 2 to 5 μM range concentration (10 mM phosphate buffer, pH 7.00, 100 mM NaCl, 1 mM EDTA) assuming identical extinction coefficient for the α,β-D-C_2NA including oligonucleotide and the corresponding unmodified ones. Melting temperatures were calculated by use of the Carry software.

Conflicts of interest

There are no conflicts to declare.

Acknowledgements

This work was granted access to the HPC resources of the CALMIP supercomputing centre (allocation p18001).

Notes and references

1 a) O. Khakshoor and E. T. Kool, *Chem. Commun.* 2011, **47**, 7018. b) Y. Morita, M. Leslie, H. Kameyama, D. E. Volk and T. Tanaka, *Cancers.* 2018, **10**, 80, 1. c) A. Rajendran, E. Nakata, S. Nakano and T. Morii, *ChemBioChem* 2017, **18**, 696. d) P. Chidchob and H. F. Sleiman, *Curr. Opin. Chem. Biol.*, 2018, **46**, 63. e) S. Li, Q. Jiang, S. Liu, Y. Zhang, Y. Tian, C. Song, J. Wang, Y. Zou, G. J. Anderson, J.-Y. Han, Y. Chang, Y. Liu, C. Zhang, L. Chen, G. Zhou, G. Nie, H. Yan, B. Ding and Y. Zhao, *Nat. Biotechnol.* 2018, **36**, 258.

2 a) A. Khvorova and J. K. Watts, *Nat. Biotechnol.* 2017, **35** (3), 238. b) N. M. Bell and J. Micklefield, *ChemBioChem*, 2009, **10**, 2691. c) Chemical synthesis of nucleoside analogues Ed.: P. Merino J. Wiley & Sons, Hoboken, **2013**. d) W. R. Algar, D. E. Prasuhn, M. H. Stewart, T. L. Jennings, J. B. Blanco-Canosa, P. E. Dawson and I. L. Medintz *Bioconjugate Chem*. 2011, **22**, 825. e) Y. Singh, P. Murat and E. Defrancq, *Chem. Soc. Rev*. 2010, **39**, 2054.

3 J. Lebreton, J.-M. Escudier, L. Arzel and C. Len, *Chem. Rev.* 2010, **110**, 3371.

4 H. Kaur, B. R. Babu and S. Maiti, *Chem. Rev.* 2007, **107**, 4672.

5 a) P. M. E. Gramlich, C. T. Wirges, A. Manetto and T. Carell, *Angew. Chem. Int. Ed*. 2008, **47**, 8350. b) C. J. Pickens, S. N. Johnson, M. M. Pressnall, M. A. Leon and C. J. Berkland *Bioconjugate Chem*. 2017, **29**, 686. c) J. Matyašovský, R. Pohl and M. Hocek, *Chem. Eur. J*. 2018, **24**, 14938.

6 a) I. K. Astakhova and J. Wengel, *Acc. Chem. Res*. 2014, **47**, 1768. b) M. Ejlersen, N. J. Christensen, K. K. Sørensen, K. J. Jensen, J. Wengel and C. Lou, *Bioconjugate Chem*. 2018, **29**, 1025.

7 a) D. J. Cram, *Angew. Chem. Int. Ed*. 1988, **27**, 1009. b) M. Tarköy and C. J. Leumann, *Angew. Chem. Int. Ed*. 1993, **32**, 1432.

8 a) C. R. Allerson, S. L. Chen and G. L. Verdine, *J. Am. Chem. Soc*, 1997, **119**, 7423. b) J.-M. Escudier, I. Tworkowski, L. Bouziani and L. Gorrichon, *Tetrahedron Lett*. 1996, **37**, 4689.

9 D.-A. Catana, B.-L. Renard, M. Maturano, C. Payrastre, N. Tarrat and J.-M. Escudier, *Journal of Nucleic Acids* 2012, 215876.

10 a) V. Banuls, J.-M. Escudier, C. Zedde, C. Claparols, B. Donnadieu and H. Plaisencié, *Eur. J. Org. Chem*, 2001, 4693. b) J. Schulz, D. Vimont, T. Bordenave, D. James, J.-M. Escudier, M. Allard, M. Szlosek-Pinaud and E. Fouquet *Chem. Eur. J*. 2011, **17**, 3096. c) C. Addiamiano, B. Gerland, C. Payrastre and J.-M. Escudier *Molecules*, 2016, **21**, 1082.

11 C. Dupouy, I. Le Clézio, P. Lavedan, H. Gornitzka, J.-M. Escudier and A. Vigroux, *Eur. J. Org. Chem.* 2006, 5515.

12 A. Boissonnet, C. Dupouy, P. Millard, M.-P. Durrieu, N. Tarrat and J.-M. Escudier, *New J. Chem.* 2011, **35**, 1528.

13 B. Gerland, P. Millard, C. Dupouy, B.-L. Renard and J.-M. Escudier, *RSC Advances* 2014, **4**, 48821.

14 B. Gerland, C. Addiamiano, B.-L. Renard, C. Payrastre, D. Gopaul and J.-M. Escudier, *Eur. J. Org. Chem.* 2017, 1450.

15 A. Kraszewski, M. Sobkowski and J. Stawinski, *J. Chem. Soc. Perkin Trans 1*, 1993, 1699.

16 I. Le Clézio, J.-M. Escudier and A. Vigroux, *Org. Lett.* 2003, **5**, 161.

17 C. Altona and M. Sundaralingam, *J. Am. Chem. Soc.* 1973, **95**, 2333.

18 M. Ikehara, *Heterocycles* 1984, **21**, 75.

19 a) D. G. Gorenstein, R. Rowell and J. Findlay, *J. Am. Chem. Soc.* 1980, **102**, 5077. b) J. M. Harrison, T. D. Inch and G. L. Lewis, *J. Chem. Soc. Perkin Trans 1*, 1975**,** 1892. c) J. P. Majoral and J. Navech, *Bull. Soc. Chim. France*, 1971, **95**, 1331.

20 P. P. Lankhorst, C. A. G. Haasnoot, C. Erkelens and C. Altona, *J. Biomol. Struct. Dyn.* 1984, **1**, 1387.

21 B. Schneider, S. Neidle and H. M. Berman, *Biopolymers*, 1997, **42**, 113.

22 A. Polyanichko and H. Wieser, *Biopolymers*, 2005, **78**, 329.

23 M. H. Caruthers, *Acc. Chem. Res.* 1991, **24**, 278.

24 C. Dupouy, N. Iché-Tarrat, M. P. Durrieu, F. Rodriguez, J.-M. Escudier and A. Vigroux, *Angew. Chem. Int. Ed*. 2006, **46**, 3623.

25 C. Dupouy, N. Iché-Tarrat, M. P. Durrieu, A. Vigroux and J.-M. Escudier, *Org. Biomol. Chem*. 2008, **6**, 2849.

26 C. Dupouy, P. Millard, A. Boissonnet and J.-M. Escudier, *Chem. Commun*, 2010, **46**, 5142.

27 M. E Østergaard, B. Gerland, J.-M. Escudier, E. E. Swayze and P. P. Seth, *ACS Chem. Biol*. 2014, **9**, 1975.

28 a) T. Efthymiou, W. Gong and J.-P. Desaulniers, *Molecules*, 2012, **17**, 12665. b) J. Dadová, M. Vrábel, M. Adámik, M. Brázdová, R. Pohl, M. Fojta and M. Hocek, *Chem. Eur. J*. 2015, **21**, 16091. c) C. Ligeour, L. Dupin, A. Marra, G. Vergoten, A. Meyer, A. Dondoni, E. Souteyrand, J.-J. Vasseur, Y. Chevelot and F. Morvan, *Eur. J. Org. Chem*, 2014, 7621.

29 A. Pusuluri, V. Krishnan, V. Lensch, A. Sarode, E. Bunyan, D. R. Vogus, S. Menegatti, H. T. Soh and S. Mitragotri, *Angew. Chem. Int. Ed*. 2019, **58**, 1437.

30 a) G. T. Hwang, *Molecules*, 2018, **23**, 124. b) V. Valsangkar, A. R. Chandrasekaran, R. Wand, P. Haruehanroengra, O. Levchenko, K. Halvorsen and J. Sheng, *J. Mater. Chem. B*, 2017, **5**, 2074.

31 a) G. Kresse and J. Hafner, *Phys. Rev. B*, 1993, **47**, 558. b) G. Kresse and J. Furthmüller, *Comput. Mater. Sci*., 1996, **6**, 15. c) G. Kresse and J. Furthmüller, *Phys. Rev. B*, 1996, **54**, 11169.

32 a) P. E. Blöchl, *Phys. Rev. B*, 1994, **50**, 17953. b) G. Kresse and D. Joubert, *Phys. Rev. B*, 1999, **59**, 1758.

33 J. Klimes, D. R. Bowler and A. Michaelides, *J. Phys. Condens. Matter*, 2010, **22**, 022201.

34 Gaussian 09, Revision D.01, M. J. Frisch, G. W. Trucks, H. B. Schlegel, G. E. Scuseria, M. A. Robb, J. R. Cheeseman, G. Scalmani, V. Barone, G. A. Petersson, H. Nakatsuji, X. Li, M. Caricato, A. Marenich, J. Bloino, B. G. Janesko, R. Gomperts, B. Mennucci, H. P. Hratchian, J. V. Ortiz, A. F. Izmaylov, J. L. Sonnenberg, D. Williams-Young, F. Ding, F. Lipparini, F. Egidi, J. Goings, B. Peng, A. Petrone, T. Henderson, D. Ranasinghe, V. G. Zakrzewski, J. Gao, N. Rega, G. Zheng, W. Liang, M. Hada, M. Ehara, K. Toyota, R. Fukuda, J. Hasegawa, M. Ishida, T. Nakajima, Y. Honda, O. Kitao, H. Nakai, T. Vreven, K. Throssell, J. A. Montgomery Jr., J. E. Peralta, F. Ogliaro, M. Bearpark, J. J. Heyd, E. Brothers, K. N. Kudin, V. N. Staroverov, T. Keith, R. Kobayashi, J. Normand, K. Raghavachari, A. Rendell, J. C. Burant, S. S. Iyengar, J. Tomasi, M. Cossi, J. M. Millam, M. Klene, C. Adamo, R. Cammi, J. W. Ochterski, R. L. Martin, K. Morokuma, O. Farkas, J. B. Foresman, and D. J. Fox, Gaussian Inc., Wallingford CT, **2016**.

35 S. Grimme, *J. Comp. Chem.* 2006, **27**, 1787.

36 A. Carvalho, M. L. Gouveia, C. Raju Kanna, S. Wärmländer, J. Platts and S. Kamerlin, *F1000 Research* 2015, **4**, 52.